Food Chemistry 434 (2024) 137277

Contents lists available at ScienceDirect

Food Chemistry

journal homepage: www.elsevier.com/locate/foodchem

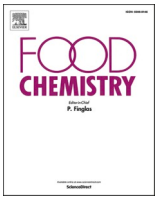

The dynamic change of flavor characteristics in Pacific oyster (*Crassostrea gigas*) during depuration uncovered by mass spectrometry-based metabolomics combined with gas chromatography-ion mobility spectrometry (GC-IMS)

Lipin Chen [a], Xiaoyu Teng [a], Yu Liu [a], Haohao Shi [a,b], Zhaojie Li [a,c,*], Changhu Xue [a,c,d,*]

[a] College of Food Science and Engineering, Ocean University of China, 1299 Sansha Road, Qingdao 266404, China
[b] College of Food Science and Technology, Hainan University, Hainan 570228, PR China
[c] Collaborative Innovation Center of Seafood Deep Processing, Dalian Polytechnic University, Dalian 116034, PR China
[d] Qingdao National Laboratory for Marine Science and Technology, Qingdao 266235, PR China

ARTICLE INFO

Keywords:
Pacific oyster (*Crassostrea gigas*)
Flavor
Depuration
Metabolome
GC-IMS

ABSTRACT

The flavor of Pacific oyster (*Crassostrea gigas*) significantly changed during the depuration process. This work aimed to explore the mechanism of flavor changes during the 72 h depuration by metabolomics combined with gas chromatography-ion mobility spectrometry (GC-IMS). The metabolomics analysis indicated that carbohydrate metabolism was more affected in the early stage of depuration, including the citrate cycle, glyoxylae and dicarboxylate metabolism, etc. After 72 h depuration, it affected mainly the metabolism of global and overview maps and nucleoside metabolism, etc. The equivalent umami concentration (EUC) value was calculated and exhibited a gradual increase following a 48 h depuration. The GC–MS results revealed that the content of furans was the highest, and the content of aldehydes, ketones, and alcohols was the lowest after 48 h depuration, while the content of aldehydes, ketones, and alcohols increased after 72 h depuration. All these results suggested the depuration period was recommended to be controlled within 48 h.

1. Introduction

As a kind of aquatic treasure, the raw Pacific oyster (*Crassostrea gigas*) is well-received among consumers for its enriched nutrients and unique flavor. Among these, the flavor is the most principal ingredient affecting consumers' acceptance. The flavor improvement of oysters has been extensively studied. Wang et al (2022) enhanced the flavor characteristics of *C. gigas* by different microalgae dies. Liu et al. (2021a) compared the biological composition and non-volatile tap active compounds in raw, high hydrostatic pressure created and steamed oysters *Crasostrea hongkongensis*. In our previous study, it was found that a change in depuration salinity also could improve the flavor of *C. gigas* (Chen et al., 2022d), but the dynamic change molecular mechanism of flavor characteristics in *C. gigas* during depuration remains unclear. On the other hand, *C. gigas*, as filter feeders, could absorb contaminants if the water environment of the product area was polluted. Currently, depuration is the most common commercial practice for shellfish products, which are placed in clean seawater, allowing the oysters to discharge contaminants from the body (Tsai, Hsiao, Weng & Liu, 2023). Therefore, this study is expected to "kill two birds with one stone", improve the flavor by low-cost method and meanwhile meet depuration requirements for food safety.

The depuration period had a significant effect on oyster quality (Bio & Nunes, 2021; Wang et al., 2023a). In our previous studies, it was also found that the activity of oysters was significantly decreased in the later stage of depuration (Chen et al., 2022c). However, there was no clear requirement for the actual depuration period at present, which varied greatly from a few hours to a few days. In some countries, the main goal of daily depuration was to determine *Escherichia coli (E.coli)* levels, and once the standard of raw eating was reached, the depuration was terminated (Lee, Lovatelli & Ababouch, 2008). The small-sized oysters needed 36 h to reach the standard of *E. coli*, whereas medium-sized oysters took only 24 h (Chinnadurai et al., 2023). However, the effect of the depuration period on the flavor was still unknown.

* Corresponding authors at: College of Food Science and Engineering, Ocean University of China, 1299 Sansha Road, Qingdao 266404, China
E-mail addresses: lizhaojie@ouc.edu.cn (Z. Li), xuech@ouc.edu.cn (C. Xue).

https://doi.org/10.1016/j.foodchem.2023.137277
Received 2 May 2023; Received in revised form 22 August 2023; Accepted 23 August 2023
Available online 26 August 2023

Many studies suggested that there was a certain relationship between flavor and metabolites (Leggio et al., 2012). Chen et al. (2022d) found that decreasing the content of hypoxanthine (Hx) could reduce the bitter substances of *C. gigas*. Sun et al. (2022) found that fatty acids were capable of transformation into volatile substances, then further leading to a heightened meat flavor. Recently, metabolomics has been extensively employed to reveal physiological and biochemical changes and flavor precursors in seafood to improve our understanding of flavor formation (Guo et al., 2023; Samuelsson, Subbaraj & Bertram, 2022). High-throughput mass spectrometry metabolomics was regarded as optimal for identifying low-molecular metabolites including nucleotides, amino acids, and their derivatives, which were more sensitive and specific for investigating molecular alterations in organisms (Qian et al., 2023; Wang et al., 2023b; Yang et al., 2021). Castro-Alves et al. (2021) unraveled metabolite signatures associated with the sensory quality of *Anethum graveolens* using metabolomics. Yang et al. (2022) revealed flavor differences between caged and cage-free chickens by transcriptomic combined with metabolomic. Gai et al. (2023) elucidated the formation mechanisms involved in the development of meat quality and flavor attributes of Beijing You chicken by metabolomics. In contrast to conventional biochemical techniques, high-throughput mass spectrometry metabolomics was capable of detecting more metabolite, and the utilization of bioinformatics analysis could facilitate the comprehension of molecular mechanisms at the metabolite level. In addition, gas chromatography-ion mobility spectrometry (GC-IMS) was an innovative methodology that incorporates GC and IMS for the rapid identification of volatile organic compounds (VOCs) (Wang et al., 2023b). Chen et al. (2023) investigated the impact of low-temperature and low-salt fermentation on the VOCs of Chinese Kohlrabi utilizing GC-IMS as a means of analysis.

Hence, this work aims to clarify the dynamic changes of flavor substances during the depuration process and finally obtained the best period to adjust the flavor in the depuration process. The nucleotides, free amino acids, and metabolomic approaches were used to analyze the small molecular metabolites in the depuration process, and the equivalent umami concentration (EUC) value was calculated. In addition, the VOCs were established by GC-IMS. Principal components analysis (PCA), orthogonal partial least squares discriminant analysis (OPLS-DA) model, and other chemometric tools were used to process the multivariate data set (Chen et al., 2022a). Beyond that, differential metabolites (DMs) were further subjected to function analysis attempting the mechanism clarification. This study would provide theoretical reference information for enhancing the quality and flavor of oyster depuration.

2. Materials and methods

2.1. Sample preparation

The live *C. gigas* from a local oyster farm in Jiaozhou Bay (Shandong province, China) were harvested and transported to the lab under low temperatures by ice. The time for transportation from the production area to the lab was < 2 h. After the *C. gigas* were cleaned, the 9 live *C. gigas* were immediately sacrificed as the Control group (label: DP-0 h). 150 *C. gigas* samples were put into depuration tanks containing artificial seawater and equipped with ultraviolet and oxygenation systems. The salinity of seawater was set at 29 g/L (corresponding to −10 % salinity fluctuation with production area) according to our previous research result (Chen et al., 2022d), which was obtained by dissolving sea salt in water. The temperature was kept at 15 ± 1°C (Chen et al., 2022b). The *C. gigas* remain in the depuration process for 72 h. The 9 live *C. gigas* were taken from depuration tanks and dissected at 24 h regular intervals, the samples were maintained at − 40 °C until analysis (label: DP-24 h, DP-48 h, DP-72 h, respectively).

2.2. Metabolomic analysis

Fifty mg *C. gigas* samples were precisely weighed and subjected to extraction utilizing a 400 μL methanol–water solution (v/v, 4:1, UPLC-MS; Thermo Fisher, USA) (Zhang et al., 2023a). The mixture was permitted to settle at −10 °C and subjected to a high-throughput tissue crusher at 50 Hz for 6 min, subsequent vortex for 30 s, and ultrasound at 40 kHz for 30 min. Following centrifugation at 13,000 *g* at 4 °C for 15 min, the resultant supernatant was meticulously transferred to sample vials and stored at − 80 °C. In addition, the pooled quality control (QC) sample was generated by combining equivalent volumes of all samples to appraise system conditioning and the quality control process, which was analyzed with the same method as the analytic samples.

Chromatographic separation of the metabolites was conducted using a Thermo UHPLC-Q Exactive Mass Spectrometer outfitted with an ACQUITY UPLC HSS T3 (100 mm × 2.10 mm i.d., 1.80 μm; Waters, Milford, USA) (Zheng et al., 2023). The mobile phases were composed of 0.1 % formic acid in 95 % water and 5 % acetonitrile (solvent A) and 0.1 % formic acid in a mixture of acetonitrile: isopropanol: water (9.5:9.5:5, v/v/v; solvent B). The solvent gradient changed according to the following conditions: from 0 to 3 min, 100 % (A): 0 % (B) to 80 % (A): 20 % (B); from 3 to 4.5 min, 80 % (A): 20 % (B) to 65 % (A): 35 % (B); from 4.5 to 5 min, 65 % (A):35 % (B) to 0 % (A): 100 % (B); from 5 to 6.3 min, 0 % (A):100 % (B) to 0 % (A): 100 % (B), from 6.3 to 6.4 min, 0 % (A): 100 % (B) to 100 % (A): 0 % (B), from 6.4 to 8 min, 100 % (A): 0 % (B) to 100 % (A): 0 % (B). The flow rate was 0.4 mL/min. The sample injection volume employed for the analysis was 3 μL, and the column temperature was set at 40 °C. The UPLC system was interfaced with a quadrupole-time-of-flight mass spectrometer (UHPLC-Q Exactive, Thermo, MA, USA) equipped with an electrospray ionization (ESI) source operated in both positive mode (pos mode) and negative mode (neg mode). The conditions were set as follows: source temperature, 425 °C; curtain gas (CUR), 30 psi; both Ion Source GS1 and GS2, 50 psi; ion-spray voltage floating (ISVF), − 3500 V in neg mode and 3500 V in pos mode; declustering potential, 80 V; 20–60 V rolling for collision energy.

Following UHPLC-QE analyses, the raw data were loaded into the Progenesis QI 2.3 (Nonlinear Dynamics, Waters, USA) to detect peak detection and alignment, which would generate a data matrix, including the retention time (RT), mass-to-charge ratio (*m/z*) values, and peak intensity information (Wan et al., 2022).

Metabolites were identified by applying accurate mass, MS/MS fragment spectra, and isotope ratio difference based on Metlin (https://metlin.scripps.edu/) and Human Metabolome Database (HMDB, http://https://www.hmdb.ca/) (Li, Luo, Zeng, Zhu, & Lu, 2022b).

2.3. Analysis of free amino acids (FAAs)

The extraction of free amino acids in *C. gigas* was performed following the established methodology described by Chen et al. (2022d). *C. gigas* were extracted using 10.00 mL 0.02 M dilute hydrochloric acid solution, then subjected to ultrasound for 5 min. The supernatant of *C. gigas* extraction was obtained after being centrifuged at 4 °C at the rate of 10,000 *g* for 10 min. The precipitate was treated again, and the two obtained supernatants were combined, then diluted to 25.00 mL with Milli-Q purified water (Millipore Sigma, USA). Subsequently, 2.00 mL of the diluent was combined with 2.00 mL of 5 % sulfosalicylic acid, followed by centrifugation. The supernatant was vialed through the filter membrane-quo system of 0.22 μm (Chen, Chen, Qiu & Li, 2013), and then analyzed with an automatic amino acid analyzer (L-8900, Tokyo, Japan).

2.4. Analysis of 5′-nucleotides

The ATP-related compounds were analyzed following the described by Chen et al. (2022d). *C. gigas* 5.00 g was homogenized in 15.00 mL of 10 % cold perchloric acid and then centrifuged for 10 min at 4 °C.

Treated again, and merged supernatants. The resulting supernatant was neutralized to pH 6.70 with potassium hydroxide, then underwent filtration through a 0.22 μm membrane, and then subjected to separation via high-performance liquid chromatography (HPLC) (Agilent Technologies Inc., Santa Clara, CA, USA) using a CAPCELLPAK C18 SG column (4.60 mm × 150 mm, Shiseido Co., ltd., Tokyo, Japan) (Wang et al., 2022). The temperature was set as 40 °C. Using an equal elution procedure, and the eluent was composed of a mixture of 20 mmol/L acetic acid, 20 mmol/L citric acid, and 40 mmol/L triethylamine. The flow rate was set to 0.80 mL/min, and the detector wavelength was set to 260 nm. The injected sample volume was 10 μL. The identification and quantification of the nucleotides were achieved by comparing the retention times and peak areas of standard compounds (99 % purity; Sigma-Aldrich, St. Louis, MO, USA).

2.5. EUC analysis

The EUC was considered as the concentration of monosodium glutamate (MSG, g/100 g) equivalent to the umami intensity generated by the umami amino acids (aspartic acid (Asp) and glutamic acid (Glu)) and 5' -nucleotides (5'-inosine monophosphate (IMP), 5'-guanosine monophosphate (GMP), and 5'-adenosine monophosphate (AMP)) (Yamaguchi, Yoshikawa, Ikeda & Ninomiya, 1971). The EUCs were calculated following the established methodology by Liu et al. (2021b): EUC (g MSG/100 g) = aibi + 1218 (aibi) (ajbj).

1218 was a synergistic constant of EUC. The parameters ai and bi represented the concentration of umami amino acids (Asp or Glu) (g/100 g) and the relative umami coefficients (RUC) were 1 and 0.077 respectively. Similarly, the parameters aj and bj denoted the concentrations of taste 5′-nucleotides (5′-IMP, 5′-AMP, 5′-GMP) (g/100 g), and the RUC were 0.18, 1, 2, respectively.

2.6. Odor components analysis by GC-IMS

The VOCs in *C. gigas* during depuration were analyzed using a Flavor Spec® model system (G.A.S., Dortmund, Germany) with FS-SE-54-CB capillary column (15.00 m × 0.53 mm, 1.00 μm) at 40 °C (Lu et al., 2022). The analysis parameters were adjusted according to our previous report (Chen et al., 2022d). 1.50 g of *C. gigas* was placed into a headspace injection bottle and incubated at 60 ℃ with agitation at 500 rpm/min, 20 min. Then, 500 μL of headspace samples were automatically injected into the injector at a spitless mode. The carrier gas was used as nitrogen carrier gas (≥99.99%). When determining volatile compounds, use *n*-ketones C4–C8 (Sinopharm Chemical Reagent Beijing Co., Ltd, China) as external references to calculate the retention index (RI) of each volatile compound, and the identification of VOCs was accomplished by comparing the retention index (RI) and drift time (DT) using the GC × IMS Library Search software (G.A.S., Dortmund, Germany).

2.7. Data processing and statistical analysis

The UHPLC-Q Exactive Mass Spectrometer raw data were analyzed by the R software package (Version 1.6.2). The DMs were screened based on the P value < 0.05 and variable importance projection (VIP) > 1.0 obtained from the OPLS-DA model (Zheng et al., 2023). The values of FAAs, nucleotides, and EUC data were presented as mean ± standard deviation (*S. D.*) and were subjected to one-way analysis of variance (ANOVA), followed by the least significant difference (LSD) test. In this study, the statistical significance was established as $P < 0.05$. The TBtools was used for data visualization (Chen et al., 2020).

3. Results and discussion

3.1. Metabolomic analysis

3.1.1. Chemometric analysis

These 610 metabolites were identified (pos mode: 451; neg mode: 159) in the *C. gigas* at depuration 0 h, 24 h, 48 h, and 72 h after the analysis of the metabolites, which included 9 categories of metabolites, lipids and lipid-like molecules, nucleosides, and analogues, organic acids and derivatives, organoheterocyclic compounds, and organic oxygen compounds. The lipids, organic acids and derivatives, nucleic acids, amino acids chemical compounds were the most abundant metabolites (Fig. 1A and B). Similarly, Brew et al. (2020) found that the amino acid and fatty acid metabolism were significantly altered in the eastern oyster (*Crassostrea virginica*) by 8 d depuration. OPLS-DA was utilized to reveal the changes in metabolites of *C. gigas*. It was observed that clear separation between each two groups, indicating significant alterations in the metabolite level of *C. gigas* across various depuration periods (Fig. 1C and D). As seen in Fig. 1C and D, along the direction of t[1], an absolute separation was observed at 0 h depuration owing to the significant modifications in the metabolite of *C. gigas* compared with that of samples after depuration. In the dimension of t[2], the metabolite pattern of 72 h depuration samples clustered completely separate from the depuration 24 h and 48 h groups. By conducting a thorough examination of three depuration periods, it was concluded that 72 h depuration resulted in significant changes in the metabolite of *C. gigas*. When *C.gigas* entered the depuration process after cleaning, the original balance of normal metabolism was disrupted. During exposure to a stressful environment, organisms undergo alterations in several metabolic pathways, including amino acid metabolism, purine metabolism, and ABC transporter pathway, among others, in response to changes in intracellular osmolarity induced by the external environment (Hosoi et al., 2003; Pedley & Benkovic, 2017). Inevitably, the content of some metabolites could be changed, as reported, under salinity stress, amino acid-related metabolisms were disorderly, including histidine, L-Ornithine, etc (Du et al., 2020).

To evaluate the differences between groups, pairwise OPLS-DA was used to filter DMs. Considering combined P-value < 0.05 and VIP values > 1.0 to screen DMs, 191 metabolites qualified as DMs (Fig. S1) between 0 h depuration and other depuration periods, and they could be divided into nine categories (Fig. S1), namely lipids and lipid-like molecules (37.69 %), organic acids and derivatives (20.77 %), nucleosides, nucleotides, and analogues (10.77 %), organoheterocyclic compounds (10.00 %), benzenoids (7.69 %), organic oxygen compounds (5.38 %) and others (7.69 %). A Venn diagram (Fig. 1E) was produced to illustrate the relationship between joint different metabolites among 0 h, 24 h, 48 h, and 72 h. As shown in Fig. 1F and Fig. S2, the numbers of DMs were 76 in 24 h depuration *vs.* 0 h depuration, 57 in 48 h depuration *vs.* 0 h depuration, 100 in 72 h depuration *vs.* 0 h depuration. The VIP and P-values of DMs were showed in Fig. 2 A, B, and C. In comparisons, 32 overlapping DMs were considered key metabolites for *C. gigas*. 72 h depuration produced more DMs, most of which were lipids and lipid-like molecules, organic acids, and derivatives, nucleosides, nucleotides, analogues, etc. Numerous metabolites were associated with flavor attributes. For example, ATP-related compounds, such as AMP, IMP, and Hx exhibited significant potential in influencing the overall flavor of oysters. Similarly, according to Du et al. (2021), the flesh quality of crucian carp was improved during different treatment periods due to the significant involvement of the TCA cycle, ornithine cycle, purine metabolism, and amino acid catabolism metabolic pathways.

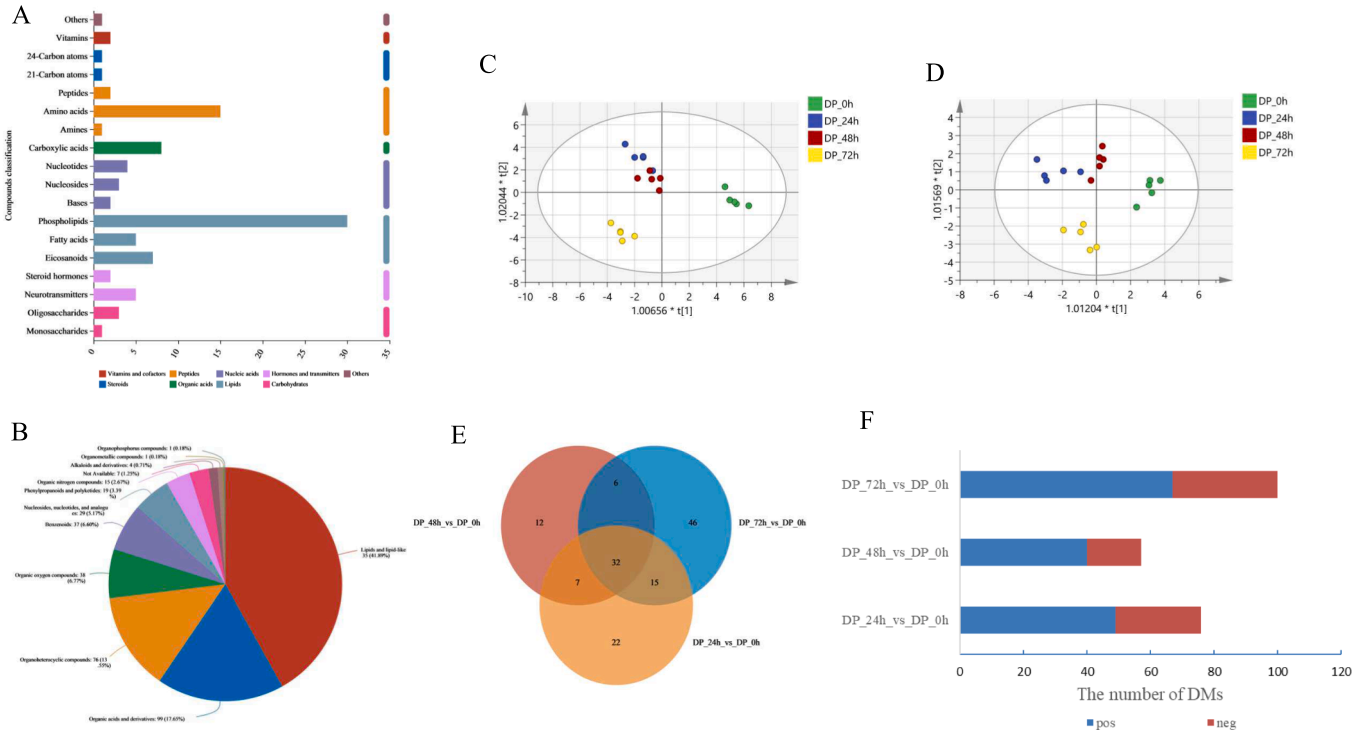

Fig. 1. Metabolomic analysis of *Crassostrea gigas* during depuration. (A) The Kyoto Encyclopedia of Gene and Genomes compounds classification of total identified metabolites; (B) The subclass classification of total identified metabolites based on Human Metabolome Database; (C) The orthogonal partial least squares discriminant analysis (OPLS-DA) analysis of *C. gigas* metabolites based on in positive modes (D) OPLS-DA analysis of *C. gigas* metabolites based on in negative modes; (E) Venn diagram showing the common and unique differential metabolites (DMs); (F) Number of DMs of *C. gigas*.

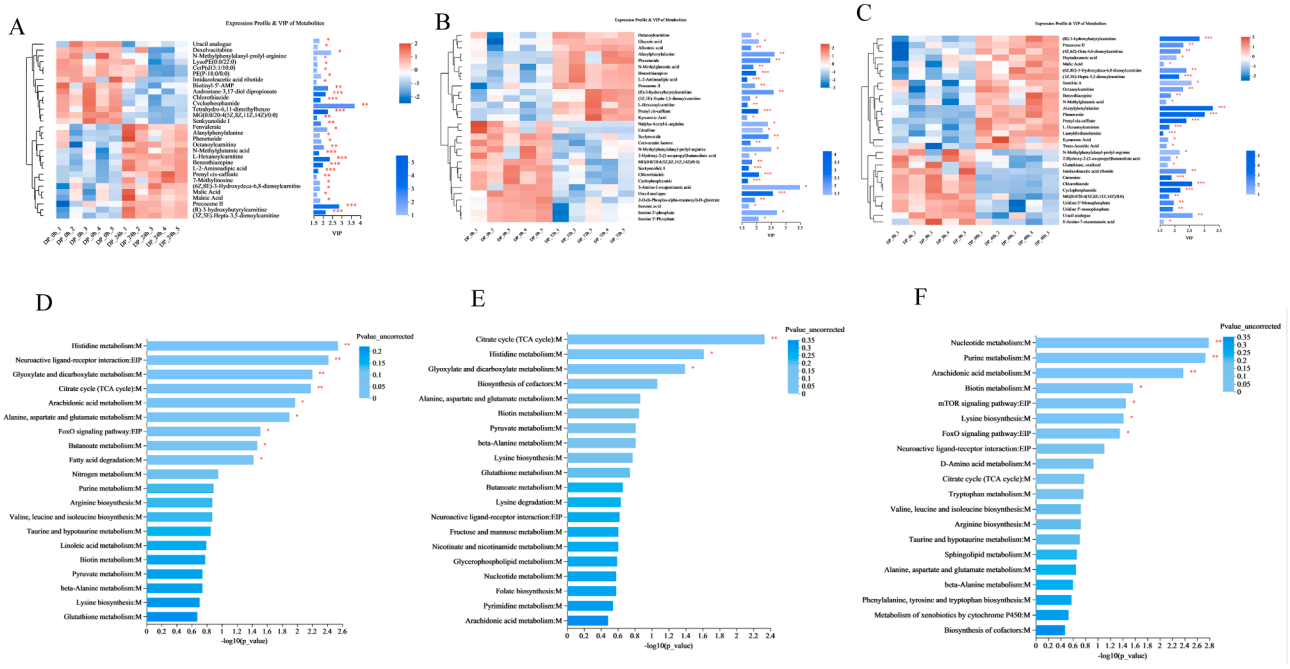

Fig. 2. (A-C) The VIP and P-Value of differential metabolites (DMs), (A) 24 h depuration *vs* 0 h depuration; (B) 48 h depuration *vs* 0 h depuration; (C) 72 h depuration *vs* 0 h depuration; The right side is the VIP bar chart of metabolites. The bar color indicates the significant difference in metabolites. Right * represents $P < 0.05$, ** represents $P < 0.01$, *** represents $P < 0.001$; (D-F) Kyoto Encyclopedia of Genes and Genomes (KEGG) analysis of DMs. (D) 24 h depuration *vs* 0 h depuration; (E) 48 h depuration *vs* 0 h depuration; (F) 72 h depuration *vs* 0 h depuration.

3.1.2. Bioinformatics analysis of DMs

Metabolomics has arisen as a crucial technique to identify endogenous metabolites including flavor substances for the quality, and safety of products (Patti, Yanes & Siuzdak, 2012). To further investigate the key pathways involved in the development of *C. gigas* flavor, KEGG pathway analysis of the DMs was performed. The results indicated that *C. gigas* reacted to the changes in metabolites after depuration and then affected the quality of *C. gigas*. To investigate the key pathways related to the metabolic response to *C. gigas* with different depuration periods, the DMs among the three depuration period samples underwent pathway analysis using Metaboanalyst 4.0. The pathway impact and P-values were presented in Fig. 2 D-F. According to the KEGG pathway enrichment analysis, the amino acid metabolic pathway was affected at every period in the depuration process, including histidine metabolism, alanine, aspartate, and glutamate metabolism. In the early stage of depuration (24 h and 48 h), carbohydrate metabolism was affected, including the citrate cycle (TCA cycle), glyoxylate and dicarboxylate metabolism, etc. At 72 h depuration, it affected the metabolism of global and overview maps, the metabolism of cofactors and vitamins, and nucleoside metabolism. Based on the content changes of DMs of *C. gigas* along with the pathway information retrieved from the KEGG database, the maintained pathways of *C. gigas* metabolism were deduced, proving valuable insights into the metabolic shifts occurring during depuration (Fig. 3). The taste development of *C. gigas* was associated to the free amino acids and nucleic acids, etc., which was consistent with Zhao et al. (2022).

3.2. Change in amino acid metabolism of C. gigas during depuration

The KEGG analysis evidenced that the amino acid metabolism pathway was significantly enriched during depuration. The main DMs during depuration were amino acids (Fig. S3), including histidine, and glutamate, which was consistent with quantitative analysis. Amino acids-related metabolisms were susceptible to salinity stress (Hosoi et al., 2003) and free amino acids were determined as the important components of taste substances of *C. gigas*. Besides salinity also could enhance the taste of aquatic products by changing the levels of specific FAAs (Chen et al., 2022d). The umami taste was associated with the aspartic acid (Asp) and glutamic acid (Glu); alanine (Ala), arginine (Arg), proline (Pro), threonine (Thr), serine (Ser), glycine (Gly) were related to the sweet taste of *C. gigas*, whereas the valine (Val); methionine (Met), isoleucine (Ile), leucine (Leu), tyrosine (Tyr), phenylalanine

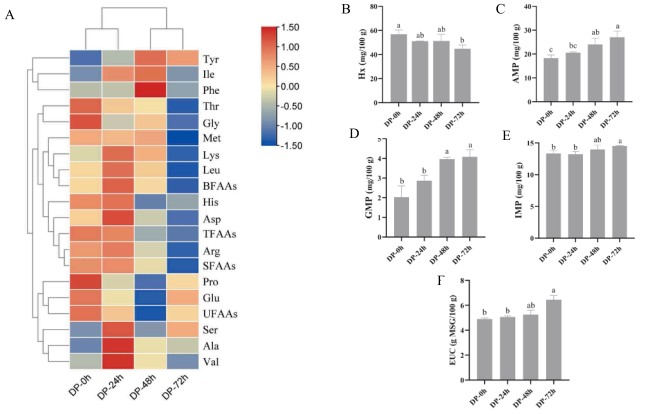

Fig. 4. The content of nucleotides and free amino acids (FAAs) in *Crassostrea gigas* during depuration. (A) The hot map for free amino acids; (B) hypoxanthine (Hx); (C) adenosine monophosphate (AMP); (D) guanosine monophosphate (GMP); (E) inosine monophosphate (IMP); (F) equivalent umami concentration (EUC).

(Phe), lysine (Lys) and histidine (His) were responsible for the bitter taste of *C. gigas* (Yuasa et al., 2018). In this study, 74 amino acids were identified by UHPLC-Q Exactive HF-X, and the contents of amino acids were significantly decreased after depuration (Fig. S3). In our previous studies, it was found that reducing bitter amino acids including His could improve *C. gigas* flavor. In the present research (Fig. 4A), the content of His showed the largest decrease at depuration 48 h, which could be responsible for the decrease in bitterness after 48 h depuration of *C. gigas* (Keska & Stadnik, 2017). Similarly, Du et al. (2020) also reported that the content of His in the grass carp (*Ctenopharyngodon idella*) was decreased during the purification procedure. Some FAAs, such as Thr, Ala, Lys, Asp, and Glu showed a synchronous decrease trend, which may be due to involvement in the osmolality regulation in *C. gigas*. Prior research indicated that the majority FAAs were decreased due to hypo-osmotic adaptation, while Pro, Arg, Gly, Ala, and Tau were increased during hyperosmotic adaptation (Hosoi et al., 2003).

Carnosine, a histidine-derived dipeptide, had been described as a taste compound, which was vitally related to the sensory characteristics of muscle foods (Zhou et al., 2021). Suyama & Shimizu (1982) reported that carnosine had a significant buffer effect. Several research studies

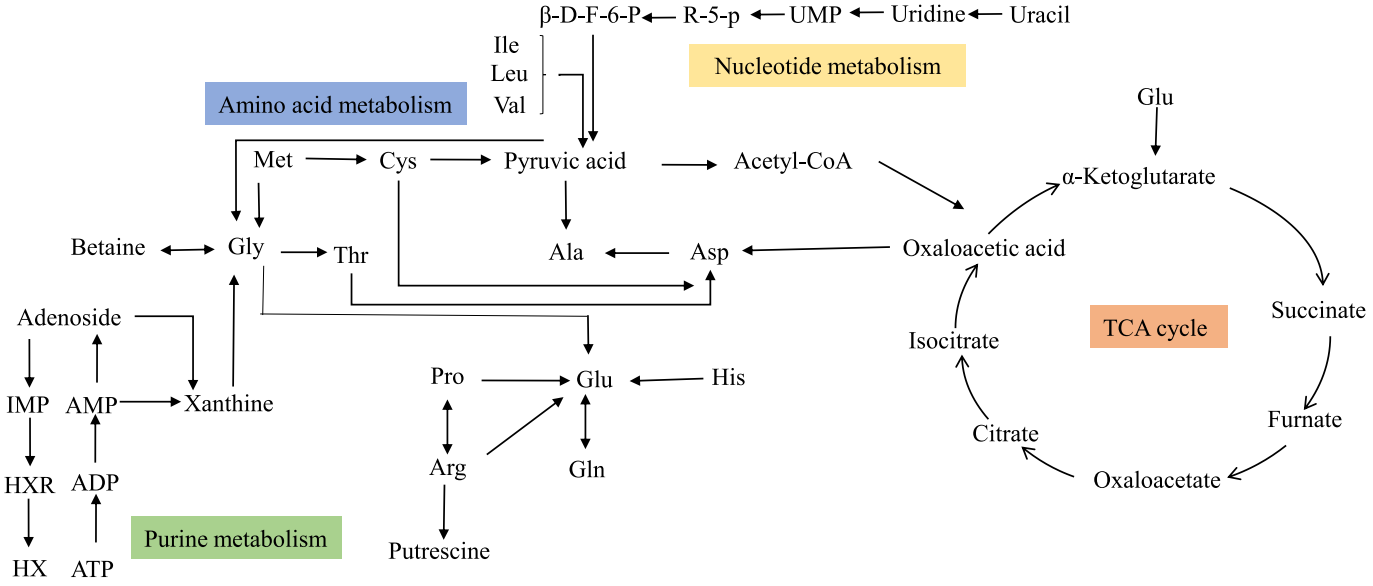

Fig. 3. The major metabolic pathways in *Crassostrea gigas* during depuration.

have reported that carnosine exhibited the potential to enhance the taste characteristics of meat products (Zhang et al., 2023b). Furthermore, carnosine could enhance the richness and prolong the taste (Dashdorj, Amna & Hwang, 2015). For example, the richness and taste attributes of beef broth were significantly enhanced by the higher content of anserine and its existence (Pereira-Lima, Ordonez, Garcia De Fernando & Cambero, 2000). The concurrent presence of anserine and carnosine in the meat resulted in a decrease in the bitterness and an increased the umami intensity (Kajiya, Arino, Koshio & Minami, 2023). In our results, it was found that the content of carnosine decreased significantly after depuration (Fig. S3), which was also related to the decrease in the richness and bitterness of *C. gigas* after depuration as shown in our previous results of the electronic tongue of taste substances (Chen et al., 2022d).

3.3. Change in carbohydrate metabolism of C. gigas during depuration

A multitude carbohydrate metabolism pathways have been observed to be enhanced in response to salinity stress, enabling improved salinity tolerance, including tricarboxylic acid (TCA) cycle and glyoxylate and dicarboxylate metabolism. Additionally, research suggested that under salinity stress, the TCA cycle generated greater energy output and expedited the physiological and metabolic response to stress (Choi, Son & Baek, 2021; Patel et al., 2022). There were 19 metabolites enriched in the TCA cycle in the present study (Fig. S4). At depuration 24 h and 48 h, the TCA cycle pathway was activated and likely the major route for supplying energy, which could explain the increase in contents of malate, citrate, and citric acid after depuration. Meantime, malic acid and citric acid were important taste substances (Zhang, 2022), which would further lead to changes in *C. gigas* flavor after depuration. In addition, TCA cycle represented the ultimate metabolic pathway for the three principal nutrients, namely carbohydrates, lipids, and amino acids, as well as the central hub for the metabolism of carbohydrates, lipids, and amino acid metabolism (Wu, Zhao, Lai & Yang, 2021). The interplay between the tricarboxylic acid (TCA) cycle significantly influenced both purine metabolism and amino acid metabolism, thereby exerting a consequential impact on flavor modulation. For instance, a notable surge in glutamine content was observed during the 24 h depuration, indicating its correlation with altered amino acid metabolism. Apart from the TCA cycle, glyoxylate and dicarboxylate metabolism pathway was also activated during depuration according to results in this study, which was conducive to maintaining enough energy supply of *C. gigas* (Li, Zheng, Sun & Xu, 2023). Additionally, this metabolic shift led to alterations in the levels of flavor-related metabolites, including malic acid, citric acid, and L-glutamic acid (Chahardoli et al., 2020). These metabolites exhibited the lowest concentration in the initial stage and displayed a subsequent increasing trend after depuration. Consequently, these changes in metabolite content could potentially enhance the flavor profile of *C. gigas*.

3.4. Change in nucleotide metabolism of C. gigas during depuration

Previous studies had reported that the degradation of adenosine triphosphate (ATP)-related compounds into 5′-nucleotides (IMP, AMP, Hx, and GMP could influence the flavor of *C. gigas* (Chen et al., 2022d). Purine nucleotides were considered fundamental building blocks of structural components of DNA and RNA molecules, act as cofactors in metabolic activities, and act as sources of ATP (Pedley & Benkovic, 2017). In the present study, 24 main metabolites were identified from nucleotide metabolism among four groups (Fig. S5). The degradation of inosine monophosphate into Hx could contribute to the bitterness of *C. gigas* (Li et al., 2022a). As seen from Fig. 4B and Fig. S5, the content of Hx showed the largest decrease at depuration 72 h ($P < 0.05$). The aforementioned outcome was in line with the previous findings of the electronic tongue (Chen et al., 2022d). Moreover, the AMP level of 48 h and 72 h depuration was higher ($P < 0.05$) (Fig. 4C), and AMP was considered as bitter taste inhibitor (Leksrisompong, Lopetcharat, Guthrie & Drake, 2012). The GMP content markedly increased after 48 h and 72 h depuration ($P < 0.05$) (Fig. 4D). It speculated that the taste of *C. gigas* would be improved after 48 h depuration. The salinity fluctuation between the depuration and production areas of *C. gigas* had the potential to induce the degradation of AMP and IMP as a means of maintaining physiological balance. This suggested that salinity stress may lead to a significant rise in energy consumption, and further improve flavor, which was consistent with previous reports (Chen et al., 2022d).

3.5. EUC analysis

The EUC value could reflect the synergistic interaction of MSG and flavor 5′-nucleotides (Liu et al., 2021b). Fig. 4F showed that the EUC of the 48 h depuration was began increased and significantly higher at 72 h depuration ($P < 0.05$), which was in accordance with our prior electronic tongue findings (Chen et al., 2022d). However, the concentration of FAAs was not maximal in 72 h depuration, potentially due to the difference in the relative umami coefficient. According to Bi et al. (2021), umami FAAs exhibited a strong correlation with the levels of energy substances such as ATP and AMP, and the EUC value was positively linked with the energy level. The EUC in the 0 h depuration was lower than that after depuration ($P < 0.05$). This outcome might be because the transport stress was greater, resulting in *C. gigas* consuming more energy, culminating in a decreased energy state. Above all, our results suggested that depuration of 48 h and 72 h could improve *C. gigas* flavor.

3.6. Change in odor component of C. gigas during depuration by GC-IMS analysis

A total of 52 volatile organic compounds (Table 1) were identified in *C. gigas* after different depuration periods by GC-IMS. Some substances with higher content contain a dimer structure. These compounds represented 8 chemical classes, including 11 alcohols, 14 aldehydes, 3 hydrocarbons, 8 ketones, 9 esters, etc. The generation of these VOCs was found to be associated with the degradation of lipids and proteins, triggered by non-enzymatic and enzymatic reactions. The primary VOCs identified in this investigation were largely congruous with those previously reported in oysters (Wang et al., 2022). It could be seen from the fingerprint spectra (Fig. 5A) that the VOCs content was the highest among the samples before depuration, it evidenced that microorganisms proliferate in the raw samples, which would result in a sequence of biochemical processes to produce a substantial quantity of VOCs. After depuration, most of the volatile substances would be reduced (Fig. 5A), which exhibited a resemblance to the outcomes of our earlier research results (Chen et al., 2022d).

After depuration, the level of furans was significantly increased, while alcohols, ethers, ketones, aldehydes, and sulfur-containing substances were remarkably decreased. However, according to the hot map (Fig. 5B), the decrease degree was the most significant after 48 h depuration. It was worth noting that there was an upward trend after 72 h depuration, which might be caused by the increase in the level of aldehydes, ketones, and alcohols due to the deterioration of water quality after 72 h depuration.

The largest peak area and type of VOCs were alcohols, which was similar to our previous results (Chen et al., 2022d). Alcohols substance usually had a mild taste, and was an important volatile compound in food, mainly from the reaction of polyunsaturated fatty acids catalyzed by lipoxygenase. In the process of depuration, the content of alcohol compounds changed markedly, including propanol, 3-methyl-1-butanol, butanol, et al. Podduturi et al. (2021) found that the depuration exhibited a reducing effect on the levels of simple alcoholic volatiles, including straight-chained and branched compounds in the fish after depuration. It may be linked to the esterification reaction of alcohol compounds and acids following depuration or the subsequent reduction

Table 1
Volatile flavor compounds detected by gas chromatography-ion mobility spectrometry (GC-IMS) in *Crassostrea gigas* during depuration.

Count	Compound	CAS#	Formula	MW	RI	Rt [*sec*]
1	2-Acetyl Furan	C1192627	$C_6H_6O_2$	110.1	1500.3	919.086
2	Acetic Acid-M	C64197	$C_2H_4O_2$	60.1	1468.9	861.515
3	E-2-Heptenal	C18829555	$C_7H_{12}O$	112.2	1322.6	595.985
4	1-Hexanol	C111273	$C_6H_{14}O$	102.2	1358.4	659.462
5	Octanal-M	C124130	$C_8H_{16}O$	128.2	1286	534.514
6	2-Methyl-1-Pentanol	C105306	$C_6H_{14}O$	102.2	1246.6	473.106
7	3-Octanone-D	C106683	$C_8H_{16}O$	128.2	1248.1	475.375
8	*N*-Amyl Alcohol	C71410	$C_5H_{12}O$	88.1	1217.4	431.122
9	Heptanal-D	C111717	$C_7H_{14}O$	114.2	1183.5	386.751
10	1-Pentanol-M	C71410	$C_5H_{12}O$	88.1	1252.6	482.046
11	3-Octanone-M	C106683	$C_8H_{16}O$	128.2	1256.4	487.918
12	E-2-Hexenal	C6728263	$C_6H_{10}O$	98.1	1221.6	436.949
13	Heptanal-M	C111717	$C_7H_{14}O$	114.2	1183.4	386.573
14	3-Pentanone	C96220	$C_5H_{10}O$	86.1	989.3	215.654
15	2-Propanol	C67630	C_3H_8O	60.1	940.9	191.969
16	2-Butanone-D	C78933	C_4H_8O	72.1	900.7	176.619
17	3-Methylbutanal	C590863	$C_5H_{10}O$	86.1	870.4	165.3
18	1-Propanol-D	C71238	C_3H_8O	60.1	1036.1	246.939
19	2-Ethylfuran	C3208160	C_6H_8O	96.1	962.7	201.587
20	Ethyl Propanoate-M	C105373	$C_5H_{10}O_2$	102.1	947.8	194.865
21	Acetone	C67641	C_3H_6O	58.1	829.8	150.119
22	Propionaldehyde	C123386	C_3H_6O	58.1	796	137.492
23	Ethyl Acetate-M	C141786	$C_4H_8O_2$	88.1	888.3	171.994
24	1-Pentanol-D	C71410	$C_5H_{12}O$	88.1	1245.9	472.017
25	1-Butanol	C71363	$C_4H_{10}O$	74.1	1140.6	338.186
26	Alpha-Phellandrene	C99832	$C_{10}H_{16}$	136.2	1157.4	356.271
27	2-Heptanone	C110430	$C_7H_{14}O$	114.2	1172.3	373.275
28	O-Xylene	C95476	C_8H_{10}	106.2	1215	427.881
29	E-2-Pentenal	C1576870	C_5H_8O	84.1	1105.7	304.406
30	Hexanal	C66251	$C_6H_{12}O$	100.2	1084.7	285.926
31	Limonene	C138863	$C_{10}H_{16}$	136.2	1178.6	380.733
32	2-Pentanone-D	C107879	$C_5H_{10}O$	86.1	942.9	192.777
33	Acetic Acid Ethyl Ester	C141786	$C_4H_8O_2$	88.1	914.1	181.625
34	Butanal-D	C123728	C_4H_8O	72.1	898.5	175.802
35	Butanal-M	C123728	C_4H_8O	72.1	868.6	164.603
36	2-Propanol	C67630	C_3H_8O	60.1	875.4	167.168
37	1-Propanol-M	C71238	C_3H_8O	60.1	1038.1	248.435
38	2-Pentanone-M	C107879	$C_5H_{10}O$	86.1	1005.7	225.684
39	2-Propenal	C107028	C_3H_4O	56.1	849.9	157.612
40	Octanal-D	C124130	$C_8H_{16}O$	128.2	1282.6	529.061
41	2-Methyl 1-Propanol	C78831	$C_4H_{10}O$	74.1	1052.5	259.431
42	Alpha-Pinene	C80568	$C_{10}H_{16}$	136.2	1035	246.144
43	2-Methylbutanal	C96173	$C_5H_{10}O$	86.1	917.1	182.727
44	Trans-2-Octenal	C2548870	$C_8H_{14}O$	126.2	1417.3	767.15
45	Ethyl Heptanoate	C106309	$C_9H_{18}O_2$	158.2	1329	607.223
46	Acetic Acid-D	C64197	$C_2H_4O_2$	60.1	1465.5	855.358
47	2-Methyl-3-Methylthiofuran	C63012975	C_6H_8OS	128.2	1357.8	658.414
48	2-Methylpropanol	C78831	$C_4H_{10}O$	74.1	1089.3	289.885
49	3-Pentanone	C96220	$C_5H_{10}O$	86.1	975.5	208.019
50	Ethyl 2-Methylbutanoate-D	C7452791	$C_7H_{14}O_2$	130.2	1013.8	231.1
51	2-Butanone-M	C78933	C_4H_8O	72.1	900.5	176.53
52	2-Hexanone	C591786	$C_6H_{12}O$	100.2	1087.9	288.657
53	Butyl Propionate	C590012	$C_7H_{14}O_2$	130.2	1158.9	357.935
54	Ethyl Acetate-D	C141786	$C_4H_8O_2$	88.1	880	168.863
55	Benzaldehyde	C100527	C_7H_6O	106.1	1514.1	944.367
56	Acetoin	C513860	$C_4H_8O_2$	88.1	1282.5	528.879
57	3-Methyl-1-Butanol	C123513	$C_5H_{12}O$	88.1	1203	411.662
58	Ethylpyrazine	C13925003	$C_6H_8N_2$	108.1	1282.9	529.409
59	E-2-Pentenal	C1576870	C_5H_8O	84.1	1104.6	303.461
60	Ethyl 2-Methylbutanoate-M	C7452791	$C_7H_{14}O_2$	130.2	1039.9	249.798
61	Ethyl Propanoate-D	C105373	$C_5H_{10}O_2$	102.1	1001.5	223.085
62	Heptanal	C111717	$C_7H_{14}O$	114.2	1155.9	354.554
63	1-Pentyl Acetate	C628637	$C_7H_{14}O_2$	130.2	1156	354.648
64	Butanoic Acid Propyl Ester	C105668	$C_7H_{14}O_2$	130.2	1151.9	350.195

D, means dimer; M, means monomer; MW, molecuar weight; RI, retention index; Rt, retention time; Dt, drift time.

of alcohol to aldehydes. Our present results suggested that depuration could inhibit the formation of alcohol. The trend of aldehydes was consistent with alcohols, and the content of propionaldehyde was highest among all aldehydes. In addition, the trend of ketone compounds was like that of aldehydes and alcohols. Although ketone compounds present milk flavor and sweet butter flavor, which could enhance the fishy smell (Shen, Huang, Zhao & Sun, 2019). Therefore, ketone compounds may bring bad flavor to depuration *C. gigas*.

Furan derivatives were formed during the initial phase of the Maillard reaction and serve as antecedents to nitrogenous heterocyclic compounds such as alkyl pyrazines (Chen et al., 2022d). They would bring caramel flavor and have a favorable impact on the *C. gigas* flavor. The content of furan was significantly increased after depuration, and the level of furan in the 48 h depuration group was highest. In general,

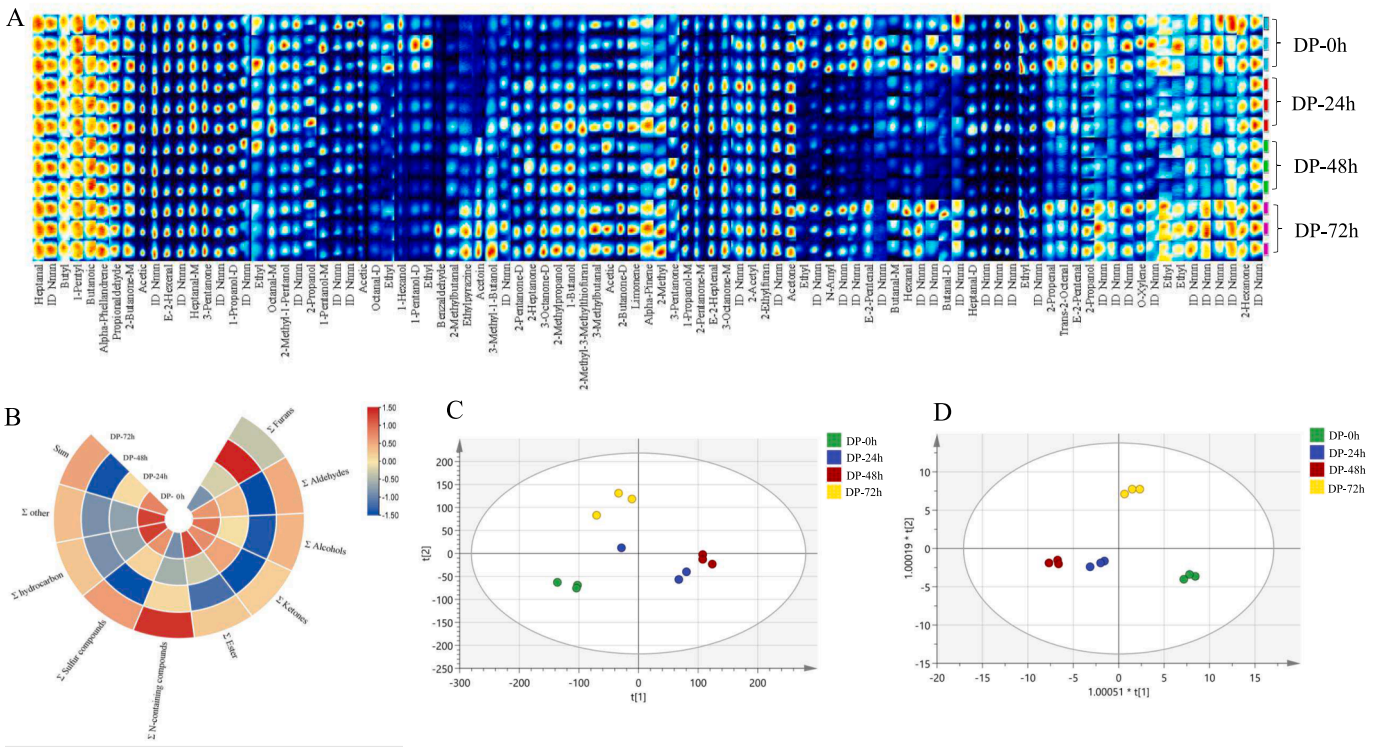

Fig. 5. Volatile organic compounds (VOCs) analysis of *Crassostrea gigas* during depuration. (A) Fingerprint spectra of VOCs based on GC-IMS; (B) The hot map for each class VOCs; (C) Principal component analysis (PCA) based on GC-IMS; (D) OPLS-DA analysis based on GC-IMS.

depuration had a dramatic impact on the lipid oxidation of *C. gigas*, and lipid oxidation was crucial to the formation of the typical aroma of meat products (Hu et al., 2021).

Furthermore, PCA/OPLS-DA analysis was performed on *C. gigas* with different depuration periods. From Fig. 5C and D, it could be seen that in the first principal component, the position of the samples between the 24 h and 48 h depuration group was close, but the 72 h depuration group was close to the raw samples. These puzzling findings might be caused by the increase in the level of aldehydes, ketones, and alcohols due to the deterioration of water quality after 72 h depuration. Therefore, it was recommended that the depuration time be controlled at 48 h.

4. Conclusion

In this study, the dynamic changes of flavor characteristics during 72 h depuration were assessed by using metabolomics combined with GC-IMS. The results showed that after 48 h depuration, the flavor of *C. gigas* began to improve via the appropriate modulation of bitter amino acid Hx and GMP, besides that, the EUC showed an increasing trend after 48 h depuration. Moreover, the results of metabolomics indicated that carbohydrate metabolism was more affected in the early stage of depuration, including TCA cycle, glyoxylate and dicarboxylate metabolism, etc. After 72 h depuration, the metabolism of global and overview maps, metabolism of cofactors and vitamins, and nucleoside metabolism were mainly affected. Furthermore, the GC-IMS results suggested that the level of furans was the highest after 48 h depuration, which was beneficial to oyster odor. Notably, the levels of aldehydes, ketones, and alcohols were the lowest after 48 h depuration, while the contents of aldehydes, ketones, and alcohols increased after 72 h depuration. In conclusion, we recommend that the depuration period be controlled at 48 h. This work would establish a theoretical framework for improving the flavor of oysters during depuration.

CRediT authorship contribution statement

Lipin Chen: Conceptualization, Data curation, Formal analysis, Funding acquisition, Investigation, Methodology, Writing - original draft,. Writing - review & editing. **Xiaoyu Teng:** Data curation, Investigation. **Yu Liu:** Conceptualization, Investigation, Methodology. **Haohao Shi:** Investigation, Methodology, Writing - original draft. **Zhaojie Li:** Conceptualization, Supervision, Writing - review & editing. **Changhu Xue:** Conceptualization, Funding acquisition, Resources, Software, Supervision.

Declaration of Competing Interest

The authors declare that they have no known competing financial interests or personal relationships that could have appeared to influence the work reported in this paper.

Data availability

Data will be made available on request.

Acknowledgments

This work was supported by the Fundamental Research Funds for the Central Universities (202161027), and earmarked fund for Modern Agro-industry Technology Research System (CARS-49).

Appendix A. Supplementary data

Supplementary data to this article can be found online at https://doi.org/10.1016/j.foodchem.2023.137277.

References

Bi, S., Chen, L., Sun, Z., Wen, Y., Xue, Q., Xue, C., … Liu, H. (2021). Investigating influence of aquaculture seawater with different salinities on non-volatile taste-active compounds in Pacific oyster (*Crassostrea gigas*). *Journal of Food Measurement and Characterization, 15*(2), 2078–2087.

Bio, S., & Nunes, B. (2021). Twists and turns of an oyster's life: Effects of different depuration periods on physiological biochemical functions of oysters. *Environmental Science and Pollution Research, 28*(23), 29601–29614.

Brew, D. W., Black, M. C., Santos, M., Rodgers, J., & Henderson, W. M. (2020). Metabolomic Investigations of the Temporal Effects of Exposure to Pharmaceuticals and Personal Care Products and Their Mixture in the Eastern Oyster (*Crassostrea virginica*). *Environmental Toxicology and Chemistry, 39*(2), 419–436.

Castro-Alves, V., Kalbina, I., Nilsen, A., Aronsson, M., Rosenqvist, E., Jansen, M. A. K., … Strid, Å. (2021). Integration of non-target metabolomics and sensory analysis unravels vegetable plant metabolite signatures associated with sensory quality: A case study using dill (*Anethum graveolens*). *Food Chemistry, 344*, Article 128714.

Chahardoli, A., Jalilian, F., Memariani, Z., Farzaei, M. H., & Shokoohinia, Y. (2020). Analysis of organic acids. In K. Eryilmaz (Ed.), *Recent advances in natural Productsanalysis* (pp. 767–823). Elsevier Inc.

Chen, C., Chen, H., Zhang, Y., Thomas, H. R., Frank, M. H., He, Y., & Xia, R. (2020). TBtools: An Integrative Toolkit Developed for Interactive Analyses of Big Biological Data. *Molecular Plant, 13*(8), 1194–1202.

Chen, H., Nie, X., Peng, T., Xiang, L., Liu, D., Luo, H., & Zhao, Z. (2023). Effects of Low-Temperature and Low-Salt Fermentation on the Physicochemical Properties and Volatile Flavor Substances of Chinese Kohlrabi Using Gas Chromatography-Ion Mobility Spectrometry. *Fermentation, 9*(2), 146.

Chen, L., Shi, H., Li, Z., Yang, F., Zhang, X., Xue, Y., … Xue, C. (2022a). Molecular mechanism of protein dynamic change in Pacific oyster (*Crassostrea gigas*) during depuration at different salinities uncovered by mass spectrometry-based proteomics combined with bioinformatics. *Food Chemistry, 394*, 133454.

Chen, L., Shi, H., Zhang, X., Xue, C., Nie, C., Yang, F., … Li, Z. (2022b). The effect of depuration salinity on the survival, nutritional composition, biochemical responses and proteome of Pacific oyster (*Crassostrea gigas*) during anhydrous living-preservation. *Food Control, 138*, Article 108977.

Chen, L., Yu, F., Shi, H., Wang, Q., Xue, Y., Xue, C., … Li, Z. (2022c). Effect of salinity stress on respiratory metabolism, glycolysis, lipolysis, and apoptosis in Pacific oyster (*Crassostrea gigas*) during depuration stage. *Journal of the Science of Food and Agriculture, 102*, 2003–2011.

Chen, L., Zhang, H., Shi, H., Xue, C., Wang, Q., Yu, F., … Li, Z. (2022d). The flavor profile changes of Pacific oysters (*Crassostrea gigas*) in response to salinity during depuration. *Food Chemistry: X, 16*, 100485.

Chen, Y. Y., Chen, S. S., Qiu, W. Q., & Li, Q. L. (2013). Identification of Different Varieties of Oyster Juice Based on the Comparison of Free Amino Acids. *Advanced Materials Research, 781–784*, 1534–1539.

Chinnadurai, S., Elavarasan, K., Geethalakshmi, V., Kripa, V., & Mohamed, K. S. (2023). Development of a depuration protocol for commercially important edible bivalve molluscs of India: Ensuring microbiological safety. *Food Microbiology, 110*, Article 104172.

Choi, I., Son, H., & Baek, J. H. (2021). Tricarboxylic Acid (TCA) Cycle Intermediates: Regulators of Immune Responses. *Life, 11*(1), 69.

Dashdorj, D., Amna, T., & Hwang, I. (2015). Influence of specific taste-active components on meat flavor as affected by intrinsic and extrinsic factors: An overview. *European Food Research and Technology, 241*(2), 157–171.

Du, H., Lv, H., Xu, Z., Zhao, S., Huang, T., Manyande, A., & Xiong, S. (2020). The mechanism for improving the flesh quality of grass carp (*Ctenopharyngodon idella*) following the micro-flowing water treatment using a UPLC-QTOF/MS based metabolomics method. *Food Chemistry, 327*, Article 126777.

Du, H., Xiong, S., Lv, H., Zhao, S., & Manyande, A. (2021). Comprehensive analysis of transcriptomics and metabolomics to understand the flesh quality regulation of crucian carp (*Carassius auratus*) treated with short term micro-flowing water system. *Food Research International, 147*, Article 110519.

Gai, K., Ge, Y., Liu, D., Zhang, H., Cong, B., Guo, S., … Sheng, X. (2023). Identification of Key Genes Affecting Flavor Formation in Beijing-You Chicken Meat by Transcriptome and Metabolome Analyses. *Foods, 12*(5), 1025.

Guo, W., Zhang, Y., Long, Z., Fu, X., & Ren, K. (2023). Study on the taste active compounds in Douchi using metabolomics method. *Food Chemistry, 412*, Article 135343.

Hosoi, M., Kubota, S., Toyohara, M., Toyohara, H., & Hayashi, I. (2003). Effect of salinity change on free amino acid content in Pacific oyster. *Fisheries Science, 69*(2), 395–400.

Kajiya, K., Arino, M., Koshio, A., & Minami, Y. (2023). Composition and taste of beef, pork, and duck meat and bioregulatory functions of imidazole dipeptides in meat. *Scientific Reports, 13*(1), 2115.

Keska, P., & Stadnik, J. (2017). Antimicrobial Peptides of Meat Origin - An In silico and In vitro Analysis. *Protein & Peptide Letters, 24*(2), 165–173.

Lee, R., Lovatelli, A., & Ababouch, L. (2008). Bivalve depuration: Fundamental and practical aspects. *FAO Fisheries Technical Paper*.

Leggio, A., Belsito, E. L., De Marco, R., Liguori, A., Siciliano, C., & Spinella, M. (2012). Simultaneous extraction and derivatization of amino acids and free fatty acids in meat products. *Journal of Chromatography a, 1241*, 96–102.

Leksrisompong, P. P., Lopetcharat, K., Guthrie, B., & Drake, M. A. (2012). Descriptive analysis of carbonated regular and diet lemon-lime beverages. *Journal of Sensory Studies, 27*(4), 247–263.

Li, D., Zhuang, S., Peng, Y., Tan, Y., Hong, H., & Luo, Y. (2022a). Mechanism of Inosine Monophosphate Degradation by Specific Spoilage Organism from Grass Carp in Fish Juice System. *Foods, 11*(17), 2672.

Li, X., Luo, J., Zeng, H., Zhu, L., & Lu, X. (2022b). Microplastics decrease the toxicity of sulfamethoxazole to marine algae (*Skeletonema costatum*) at the cellular and molecular levels. *Science of the Total Environment, 824*, 153855.

Li, Q., Zheng, Y., Sun, Y., & Xu, G. (2023). Resveratrol attenuated fatty acid synthesis through MAPK-PPAR_pathway in red tilapia. *Comparative Biochemistry and Physiology Part C: Toxicology & Pharmacology, 268*(5), Article 109598.

Liu, C., Ji, W., Jiang, H., Shi, Y., He, L., Gu, Z., & Zhu, S. (2021a). Comparison of biochemical composition and non-volatile taste active compounds in raw, high hydrostatic pressure-treated and steamed oysters *Crassostrea hongkongensis*. *Food Chemistry, 344*, 128632.

Liu, H., Ma, J., Pan, T., Suleman, R., Wang, Z., & Zhang, D. (2021b). Effects of roasting by charcoal, electric, microwave and superheated steam methods on (non) volatile compounds in oyster cuts of roasted lamb. *Meat Science, 172*, 108324.

Lu, K., Liu, L., Zi, J., Song, L., & Xie, W. (2022). New insights from flavoromics on different heating methods of traditional fermented shrimp paste: The volatile components and metabolic pathways. *LWT, 168*, Article 113880.

Patel, M. K., Pandey, S., Tanna, B., Alkan, N., & Mishra, A. (2022). Comparative metabolomics unveils the role of metabolites and metabolic pathways in the adaptive mechanisms of shrubby halophytes. *Environmental and Experimental Botany, 202*, Article 105030.

Patti, G. J., Yanes, O., & Siuzdak, G. (2012). Innovation: Metabolomics: The apogee of the omics trilogy. *Nature Reviews Molecular Cell Biology, 13*(4), 263–269.

Pedley, A. M., & Benkovic, S. J. (2017). A New View into the Regulation of Purine Metabolism: The Purinosome. *Trends in Biochemical Sciences, 42*(2), 141–154.

Pereira-Lima, C. I., Ordonez, J. A., Garcia De Fernando, G. D., & Cambero, M. I. (2000). Influence of heat treatment on carnosine, anserine and free amino acid composition of beef broth and its role in flavour development. *European food research & technology, 210*(3), 165–172.

Podduturi, R., Petersen, M. A., Vestergaard, M., Hyldig, G., & Jorgensen, N. (2021). Case study on depuration of RAS-produced pikeperch (*Sander lucioperca*) for removal of geosmin and other volatile organic compounds (VOCs) and its impact on sensory quality. *Aquaculture, 530*, 735754.

Qian, G., Wang, M., Wang, X., Liu, K., Li, Y., Bu, Y., & Li, L. (2023). Integrated Transcriptome and Metabolome Analysis of Rice Leaves Response to High Saline-Alkali Stress. *International Journal of Molecular Sciences, 24*(4), 4062.

Samuelsson, L. M., Subbaraj, A., & Bertram, H. C. (2022). Metabolomics in relation to meat quality. *New Aspects of Meat Quality (Second Edition)*, 433–460.

Shen, H., Huang, M., Zhao, M., & Sun, W. (2019). Interactions of selected ketone flavours with porcine myofibrillar proteins: The role of molecular structure of flavour compounds. *Food Chemistry, 298*, Article 125060.

Sun, A., Wu, W., Soladoye, O. P., Aluko, R. E., Bak, K. H., Fu, Y., & Zhang, Y. (2022). Maillard reaction of food-derived peptides as a potential route to generate meat flavor compounds: A review. *Food Research International, 151*, Article 110823.

Suyama, M., & Shimizu, T. (1982). Buffering Capacity and Taste of Carnosine and Its Methylated Compounds. *Nippon Suisan Gakkaishi, 48*(1), 89–95.

Tsai, H., Hsiao, Y., Weng, Y., & Liu, J. (2023). Sustainable Utilization Technology for Improving the Freshness of Oysters-Development of Alkaline Electrolysis Seawater Depuration System. *Sustainability, 15*(1), 785.

Wan, X., Zeng, W., Zhang, D., Wang, L., Lei, M., & Chen, T. (2022). Changes in the concentration, distribution, and speciation of arsenic in the hyperaccumulator *Pteris vittata* at different growth stages. *Science of the Total Environment, 841*, Article 156708.

Wang, Q., Sun, C., Chen, L., Shi, H., Xue, C., & Li, Z. (2022). Evaluation of microalgae diets on flavor characteristics of Pacific oysters (*Crassostrea gigas*) during fattening. *Food Chemistry, 391*, Article 133191.

Wang, Y., Liu, Z., Chen, X., Zhou, L., Sun, X., Yu, T., … Wu, B. (2023a). Identification and Characterization of GYS and GSK3β Provides Insights into the Regulation of Glycogen Synthesis in Jinjiang Oyster Crassostrea ariakensis. *Fishes, 8*(2), 65.

Wang, Z., Mi, S., Wang, X., Mao, K., Liu, Y., Gao, J., & Sang, Y. (2023b). Characterization and discrimination of fermented sweet melon juice by different microbial strains via GC-IMS-based volatile profiling and chemometrics. *Food Science and Human Wellness, 12*(4), 1241–1247.

Wu, J., Zhao, L., Lai, S., & Yang, H. (2021). NMR-based metabolomic investigation of antimicrobial mechanism of electrolysed water combined with moderate heat treatment against *Listeria monocytogenes* on salmon. *Food Control, 125*, Article 107974.

Yamaguchi, S., Yoshikawa, T., Ikeda, S., & Ninomiya, T. (1971). Measurement of the relative taste intensity of some l-α-amino acids and 5′-nucleotides. *Journal of Food Science, 36*(6), 846–849.

Yang, C., Zeng, Y., Liao, Y., Deng, Y., Du, X., & Wang, Q. (2021). Integrated GC–MS- and LC–MS-Based Untargeted Metabolomics Studies of the Effect of Vitamin D3 on Pearl Production Traits in Pearl Oyster *Pinctada fucata martensii*. *Frontiers in Molecular Biosciences, 8*, Article 614404.

Yang, L., Yuan, F., Rong, L., Cai, J., Yang, S., Jia, Z., & Li, S. (2022). Transcriptomic and Metabolomic Profile Analysis of Muscles Reveals Pathways and Biomarkers Involved in Flavor Differences between Caged and Cage-Free Chickens. *Foods, 11*(18), 2890.

Yuasa, M., Kawabeta, K., Eguchi, A., Abe, H., Yamashita, E., Koba, K., & Tominaga, M. (2018). Characterization of taste and micronutrient content of rock oysters (*Crassostrea nippona*) and Pacific oysters (*Crassostrea gigas*) in Japan. *International Journal of Gastronomy and Food Science, 13*, 52–57.

Zhang, L., Liang, L., Qiao, K., Pu, D., Sun, B., Zhou, X., & Zhang, Y. (2023b). Decoding the Effect of Age on the Taste Perception of Chicken Breast Soup Based on LC-QTOF-MS/MS Combined with a Chemometric Approach. *Foods, 12*(3), 674.

Zhang, Y. (2022). Recent Progress in the Study of Taste Characteristics and the Nutrition and Health Properties of Organic Acids in Foods. *Foods, 11*, 3408.
Zhang, J., Fu, B., Li, Y., Sun, J., Xie, J., Wang, G., … Yu, E. (2023a). The effect of nitrite and nitrate treatment on growth performance, nutritional composition and flavor-associated metabolites of grass carp (*Ctenopharyngodon idella*). *Aquaculture, 562*, 738784.
Zhao, X., Peng, J., Wu, H., Zheng, G., Guo, M., Kang, X., & Tan, Z. (2022). Bimonthly variation in nutrient composition and taste components of *Crassostrea gigas* cultured in Rushan, Southern yellow sea. *Aquaculture Research, 53*(18), 6711–6720.
Zheng, Z., An, Z., Yang, Y., Chen, J., Liu, X., & Lu, L. (2023). Metabolic profiling of blueberries (Vaccinium Spp.) to quantitatively and qualitatively assess bruise damage and fruit deterioration. *Postharvest Biology and Technology, 195*, Article 112135.
Zhou, C., Bai, Y., Wang, C., Li, C., Xu, X., Pan, D., … Zhou, G. (2021). 1H NMR-based metabolomics and sensory evaluation characterize taste substances of Jinhua ham with traditional and modern processing procedures. *Food Control, 126*, Article 107873.